CHAPTER 8

The Relationship Between Applied Energy and Ablation Zone Volume in Patients with Hepatocellular Carcinoma and Colorectal Liver Metastasis

Wouter J. Heerink
A. Millad Solouki
Rozemarijn Vliegenthart
Simeon J.S. Ruiter
Egbert Sieders
Matthijs Oudkerk
Koert P. de Jong

Published in European Radiology
2018, Volume 28, Issue 8, pp 3228-3236

Abstract

Objectives

To study the ratio of ablation zone volume to applied energy in computed tomography (CT)-guided radiofrequency ablation (RFA) and microwave ablation (MWA) in patients with hepatocellular carcinoma (HCC) in cirrhotic liver and colorectal liver metastasis (CRLM).

Methods

Forty-five HCCs in cirrhotic livers and 45 CRLMs were treated with RFA or with one of two MWA devices (MWA_A and MWA_B); resulting in 15 procedures for each tumor type, per device. Device settings were registered and applied energy was calculated. Ablation volume was segmented on the one-week post-procedural contrast-enhanced CT scan. The ratio of ablation zone volume to applied energy R(AZ:E) was determined for each procedure and compared between HCC (R_{HCC}) and CRLM (R_{CRLM}), stratified by ablation device.

Results

For RFA, R_{HCC} and R_{CRLM} were 0.22 (0.14-0.45) mL/kJ and 0.15 (0.14-0.22) mL/kJ (p=0.110), respectively. For MWA_A, R_{HCC} was 0.81 (0.61-1.07) mL/kJ and R_{CRLM} was 0.43 (0.35-0.61) mL/kJ (p=0.001). For MWA_B, R_{HCC} was 0.67 (0.41-0.85) mL/kJ and R_{CRLM} was 0.43 (0.35-0.61) mL/kJ (p=0.040).

Conclusions

For RFA, there was no significant difference in energy deposition ratio between tumor types. For both MWA devices, this ratio was higher for HCCs. Tailoring microwave ablation device protocols to tumor type might prevent incomplete ablations.

Introduction

For over fifteen years, hepatic malignancies have been treated successfully with radiofrequency ablation (RFA) and microwave ablation (MWA) [1–3]. The most important drawback of thermoablative therapies is recurrence of disease at the ablation site, with reported recurrence rates of 5.0-32.1% [2, 4–6]. Independent risk factors for incomplete ablation and ablation site recurrence are larger tumor size, proximity of peritumoral vessels, improper placement of ablation needle, and insufficient safety margin around the liver tumor [7–9].

To ensure complete coverage of the liver tumor including a safety margin, the creation of a predictable ablation zone is crucial. Ablation protocols provided by manufacturers are mostly based on *ex-vivo*, non-perfused, non-diseased animal experiments. It can be expected that the resulting ablation zones in these livers differ significantly from ablation zones after *in-vivo* treatment of human, diseased livers. Studies investigating the reproducibility and reliability of RFA and MWA in different tumor types and in abnormal underlying liver parenchyma (cirrhosis) in humans are lacking.

We designed this study to evaluate the ablation zone volume after RFA or MWA. The aims of this study were: 1) to find the relation between the amount of applied energy and the resulting ablation zone volume for RFA and MWA devices during human *in-vivo* ablation; and 2) investigate whether the ratio of ablation zone volume to applied energy differs between hepatocellular carcinoma (HCC) in cirrhotic livers and colorectal liver metastasis (CRLM).

Materials and methods

Patients

The study was approved and the need for informed consent was waived by the Institutional Review Board of the University Medical Center Groningen (nr. 2015/521). Data were processed anonymously. Thermoablation of liver tumors was introduced in 2000 in our hospital, ultrasound-guided during open surgery, as well as CT-guided during percutaneous procedures. Over 600 ablation procedures (approximately 70% percutaneously) have been performed for various types of liver tumors in our hospital. In the present study we analyzed only patients who underwent percutaneous CT-guided thermoablation for either CRLM or HCC in the period from March 2009 until January 2016. All patients were discussed in a tumor board meeting in which the decision for percutaneous thermoablation was made. Patients were included in this study if they were treated for HCC in a cirrhotic liver or for CRLM. Patients were excluded if: 1) there was overlap between ablation zones of multiple lesions, 2) the tumor had previously been treated with ablation therapy, or 3) surgical clips caused beam hardening on the control CT images preventing adequate segmentation of the ablation zone. For each of the three ablation devices used, 30 ablation treatments were included: 15 tumors in patients consecutively treated for HCC, and 15 tumors in patients consecutively treated for CRLM. In this paper we adhered to the standard terminology and reporting criteria as advised by Ahmed [10].

Procedure

Procedures were performed by one of two (KJ and ES) surgeons with 16 and 12 years of experience in liver ablation, respectively, with support of a radiologist. All procedures were performed under general anesthesia. Procedural CT scans and needle manipulations were performed during maximal expiration and after full elastic recoil of the thorax. This situation was obtained when CO_2 monitoring of the exhaled breathing air in the respiratory tube revealed a completely flat baseline. Thermoablation was performed with one of three devices (see below), and manufacturer's protocols were followed. Device settings were registered during the procedures. Needle placement was performed based on the expected ablation zone size described by the manufacturer, considering sufficient (>5mm) safety margin around the tumor. Larger lesions were treated by creating several partially overlapping ablation zones. After treatment of the tumor, the ablation needle was removed while performing tract ablation.

CT scan protocol

Control CT scans were acquired one week after the ablation procedure on a 64-multidetector CT system (Somatom Sensation 64, Siemens Medical, Erlangen, Germany). Tube voltage was 120 kVp and quality reference tube current was 120 mAs. Scans were acquired prior to admission of intravenous contrast agent (110 mL of Iomeron 300, Bracco Imaging), and in arterial and portal venous phase and reconstructed with 2-5mm, 0.75-3mm and 2mm slice thickness, respectively, using a medium smooth B30f kernel.

Ablation Systems

The RFA system consisted of a 480 kHz generator, with a maximum power output of 250 Watt (RF 3000 generator with Leveen needles, Boston Scientific Corp., Natick, USA). The RFA needle electrodes with umbrella arrays ranged from 2 to 5 cm in diameter. The diameter of the needle electrodes was determined by the size of the tumor. MWA system A consisted of a 2.45 GHz generator generating a maximum of 140 Watt with water-cooled needle electrodes (Acculis Sulis VpMTA; Microsulis Medical, Denmead, England). MWA system B also utilized the 2.45 GHz frequency band, generating a maximum of 100 Watt, with water-cooled needles and thermal-, field-, and wavelength-control to optimize the predictability of the ablation zone (Emprint MWA Generator; Covidien, Dublin, Ireland).

Ablation protocols and applied energy

The manufacturer of the RFA system provided separate algorithms for each of the various needle diameters, prescribing time and power settings during the procedure. The power of the system was manually increased according to this algorithm until *roll-off* was achieved. *Roll-off* is defined as a steep rise of tissue impedance, and is an indication of a successful ablation cycle. For each tumor two complete ablation cycles were generated according to the manufacturers' algorithm. During the RFA procedure, the time required to achieve *roll-off* and the *roll-off* indication power were recorded for each ablation cycle. These measurements were used to determine the area under the curve for time and power, resulting in the amount of energy applied for each ablation cycle. Next, the total amount of applied energy for each tumor was determined by summing the applied energy of all ablation cycles.

The manufacturers of MWA systems A and B provided tables with specific power and time settings according to the expected resulting ablation size. Appropriate settings were chosen, and these were recorded during the procedures. The power and time settings were used to determine the amount of applied energy for each ablation cycle, and subsequently summed per lesion to determine the total amount of applied energy.

Ablation Zone Volumetry

Volumetry of the ablation zone was performed on the portal venous phase acquisition with 2 mm slice reconstruction, using the semi-automatic *Liver Lesion Segmentation* tool (MM Oncology package, Syngo.via, Siemens Medical, Erlangen, Germany). After initial manual measurement of the tumor's cross section, this tool automatically delineated the tumor, which was subsequently verified for each slice and -when necessary- were corrected by two independent observers (WH and MS). The inter-observer reliability of volumetry was expressed as intra-class correlation coefficient (ICC). An ICC value larger than 0.90 was considered as high agreement. In ten cases with a volume discrepancy between both observers of more than ten percent, agreement of delineation between ablation zone and perilesional enhancement was checked in a consensus meeting of both observers, and was subsequently obtained by consensus. For the other ablation zones, the mean ablation zone volume from both readers was used for statistical analysis. The ratio of ablation zone volume to applied energy R(AZ:E) was determined by dividing the ablation zone volume by the amount of energy applied for each procedure.

The tumor size was determined as the largest diameter on pre-procedural contrast enhanced transverse CT images, acquired minutes before the ablation procedure. The tumor volume as a percentage of the total ablation zone volume was calculated by dividing the estimated tumor volume (based on diameter, assuming the lesions were spherical) by the total ablation zone volume. Ablations were considered incomplete when the control CT scan after one week revealed that the ablation zone did not completely cover the tumor including at least 5 mm margin around the tumor in all directions. Tumors were categorized in potential 'high' versus 'low' heat sink dependent, based on peritumoral vascularity. 'High' was defined as the presence of tumor-abutting vessels with a diameter of ≥3 mm, as defined earlier [8].

Statistical analysis

Patient age, lesion size, peritumoral vascularity, ablation time, applied energy, number of ablation needle positions, ablation zone volume, energy deposition ratio, tumor percentage in ablation zone volume, and number of incomplete ablations were compared between the three ablation devices and between tumor types, stratified per ablation device. R(AZ:E) was compared between tumor types using the Mann-Whitney U test. For each device, R(AZ:E) of potentially high and low heat sink dependent tumors were compared. Potential correlation between peritumoral vascularity and tumor type was checked using the Chi square test. For RFA, the effect the size of the needle's umbrella array on R(AZ:E) was tested using the Spearman rank test and median array diameter was compared between HCC and CRLM. R(AZ:E) of CRLMs that did receive prior systemic therapy were compared with those that did not. Parameters were tested for normality using the Shapiro-Wilk test. The mean and standard deviation (SD) of continuous, normally distributed parameters were determined and compared using one-

way ANOVA or the Independent-Samples t-test. The median and interquartile range (IQR) of non-normally distributed variables were determined and tested for homogeneous non-normality and compared using the Kruskal-Wallis or Mann-Whitney U test. Dichotomous data were compared using the Fisher Exact test. P-level was set at p=0.05 and not adjusted for multiple comparisons. Statistical analyses were performed using IBM SPSS Statistics version 23 (IBM Corporation, Chicago, USA).

Results

Patients and Procedures

In total, 90 liver tumors in 78 patients were included in this study. Thirty-five patients (27 male; median age: 67 years, IQR: 15) were treated for 45 HCCs with a mean diameter of 25.0 mm (SD: 9.6), ranging from 6 to 55 mm. Forty-three patients (26 male; median age: 64, IQR 12) were treated for 45 CRLMs with a mean diameter of 22.5 mm (SD: 10.6), ranging from 7 to 60 mm. In total, 14 tumors between 30 mm and 40 mm in size, and 4 larger than 40 mm were included. These larger tumors were treated with thermoablation because for these patients no other form of therapy was available. Seventeen patients have received prior systemic chemotherapy, with a mean of 1.1 years between chemotherapy and ablation. None of the tumors have been treated with trans-arterial (chemo) embolization.

All 90 tumors were treated in 80 sessions. In 14 tumors (15.5%) the ablation was incomplete. The median ablation zone volume for all tumors was 55.7 mL (IQR: 55.9). The inter-observer correlation for volumetry of ablation zone was high (ICC = 0.994; 95% CI: 0.990-0.996; p<0.001).

Comparison of devices

Table 1 displays baseline patient and tumor variables for each ablation device. In general, median ablation time was longer for RFA than for MWA devices (T_{RFA} = 48 min, T_{MWA_A} = 14 min, T_{MWA_B} = 20 min; p<0.001). Also, median applied energy was higher

Table 1. Patient and tumor characteristics

Generator	RFA	MWA A	MWA B	p-value
R(AZ:E) (mL/kJ)	0.17 (0.14-0.26)	0.66 (0.37-0.86)	0.46 (0.37-0.77)	<0.001
Number of lesions	30	30	30	
Patients	24	28	26	
Gender (male/female)	19/5	19/9	15/11	0.072
Age (years)	64.3 (7.7)	66.4 (11.2)	65.8 (12.1)	0.741
Lesion diameter (mm)	21.3 (7.2)	25.8 (12.6)	24.1 (9.8)	0.380
Ablation time (min)	48 (21-75)	14 (4-23)	20 (11-29)	<0.001
Applied energy (kJ)	294.0 (83.5-504.5)	111.0 (38.1-183.9)	111.0 (52.9-169.2)	0.001
Ablation volume (mL)	49.4 (23.8-75.2)	63.9 (35.9-92.0)	69.0 (25.6-112.4)	0.364
Needle positions (n)	4 (1)	4 (5)	3.5 (2)	0.535
Tumor % of total ablation zone volume	9.4 (3.4-15.4)	14.0 (3.0-25.0)	11.5 (1.5-21.5)	0.516
Previous systemic therapy	7	5	5	0.611
Incomplete ablations after one week follow-up (n)	4	7	3	0.118

*Normally distributed data are presented as mean (SD) and non-normally distributed data are presented as median (Q1-Q3); R(AZ:E) = ratio of ablation zone volume to applied energy.

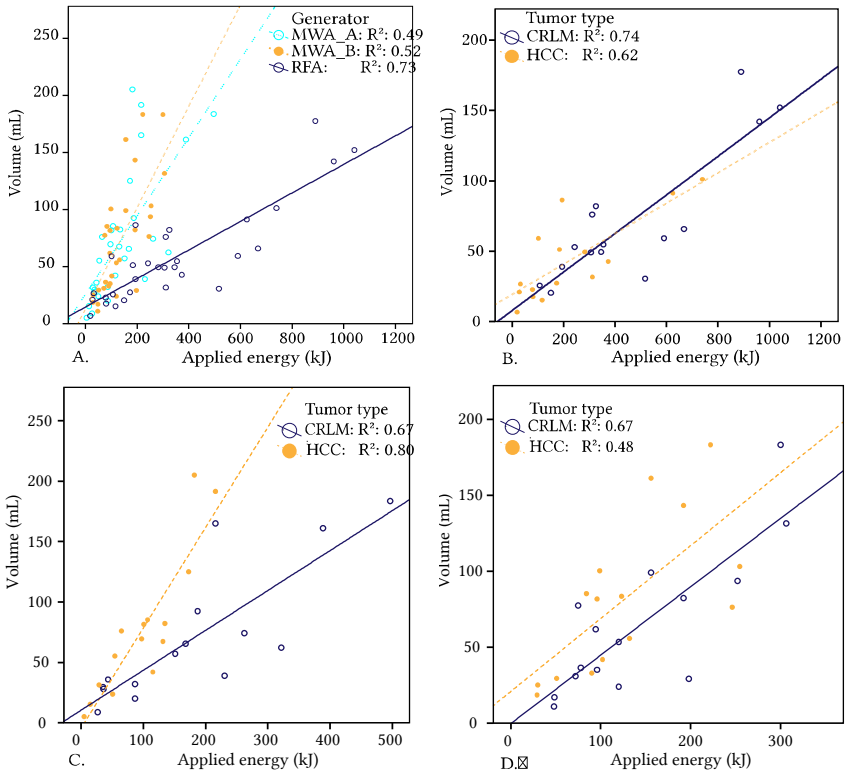

Fig 1. Regression analysis of the relationships between applied energy and (a) ablation zone volume for the three devices, (b) ablation zone volume obtained with the RFA device (Boston Scientific Corp.) grouped by tumor type, (c) ablation zone volume obtained with the MWA device A (Microsulis Medical) grouped by tumor type, and (d) ablation zone volume obtained with the MWA device B (Covidien) grouped by tumor type (CRLM colorectal liver metastasis, HCC hepatocellular carcinoma)

for RFA (E_{RFA} = 294.0 kJ, E_{MWA_A} = 111.0 kJ, E_{MWA_B} = 111.0 kJ; p=0.001). Ablation zone volume, number of needle positions, percentage tumor volume and number of incomplete ablations were approximately similar for all devices. The ablated tumor volume as a percentage of the total ablated volume was remarkably low, with a median value of 11.2% (IQR: 5.1-23.1%). R(AZ:E) was lower for RFA than for MWA devices (R_{RFA} = 0.17, R_{MWA_A} = 0.66, R_{MWA_B} = 0.46; p<0.001). Comparing this ratio between MWA devices A and B showed no significant difference (p=0.344).

For RFA, the needle's array size was correlated with R(AZ:E) with a Spearman's correlation of -0.415 (p=0.023); larger needle arrays result in a lower R(AZ:E). The median needle array size was similar for HCC and CRLM, with 3.5 cm and 3.5 cm (p=0.337), respectively.

Prior systemic therapy did not have a significant effect on R(AZ:E) for any of the devices. For RFA, median (IQR) R(AZ:E) of CRLMs that did and did not receive prior systemic therapy was 0.14 (0.10-0.20) and 0.18 (0.15-0.23; p=0.083), respectively. For MWA_A,

median R(AZ:E) was 0.34 (0.21-0.80) and 0.38 (0.34-0.56; p=0.713), and for MWA B this was 0.35 (0.17-0.75) and 0.43 (0.37-0.62; p=0.391), respectively.

Comparison of HCC with CRLM

Table 2 shows the clinicopathological and procedural characteristics, separately for HCC and CRLM, stratified for the type of ablation device used. The tumor diameter, number of peritumoral vessels, needle positions and incomplete ablations did not differ between tumor types, for any of the devices.

For RFA, R(AZ:E) did not differ significantly between tumor types (R_{HCC} = 0.22, R_{CRLM} = 0.15; p=0.110). For both MWA devices, R(AZ:E) was higher for HCC compared to CRLM: MWA_A, R_{HCC} = 0.81, R_{CRLM} = 0.43 (p=0.001), and MWA_B, R_{HCC} = 0.67, R_{CRLM} = 0.43 (p=0.040). Thus, microwave ablation generates larger ablation zone volumes per kJ in HCC as compared to in CRLM. Figure 1 shows the applied energy versus the ablation zone volume in grouped scatter plots grouped by generator, and grouped by tumor type, stratified by generator.

As an illustrative example, figure 2 shows images of an HCC and a CRLM prior to ablation with microwave device B and images of the resulting ablation zone volumes. In both these cases, 96 kJ of energy was applied, yet the resulting ablation zone volume for HCC was over twice as larger compared to CRLM.

There was no correlation between heat-sink and tumor type for RFA, MWA A and MWA B (p=0.682, p=0.466, p=0.245, respectively). Comparing R(AZ:E) of 'high' versus 'low' heatsink dependent tumors revealed no difference for RFA (R_{high} = 0.20, IQR: 0.15-0.24, R_{Low} = 0.16, IQR: 0.13-0.28, p=0.743). For MWA A, the 'high' heatsink dependent tumors resulted in a lower ratio (R_{high} = 0.39, IQR: 0.33-0.76, R_{low} = 0.83, IQR: 0.47-1.06, p=0.016), and for MWA B there was no difference in R(AZ:E) between types of tumor vascularity (R_{high} = 0.55, IQR: 0.40-0.89, R_{low} = 0.46, IQR: 0.37-0.65, p=0.422). Thus, only MWA A creates smaller ablation zone volumes in the presence of peritumoral vessels ≥3 mm, whereas the other two devices seem to be less influenced by these vessels with respect to ablation zone volume.

Table 2. Clinicopathological and procedural characteristics of HCC and CRLM according to ablation device

	RFA			MWA_A			MWA_B		
Tumor type	HCC	CRLM	p-value	HCC	CRLM	p-value	HCC	CRLM	p-value
R(AZ:E) (mL/kJ)	0.22 (0.14-0.45)	0.15 (0.14-0.22)	0.110	0.81 (0.61-1.07)	0.43 (0.35-0.61)	0.001	0.67 (0.41-0.85)	0.43 (0.35-0.61)	0.040
Tumor diameter (mm)	23.2 (5.6)	19.4 (8.2)	0.227	27.9 (12.0)	23.7 (13.2)	0.377	23.8 (10.1)	24.5 (9.9)	0.722
Peritumoral vessels >3mm	3	5	0.682	6	9	0.466	7	3	0.245
Ablation time (min)	40 (22)	76 (38.2)	0.007	13 (9)	21 (14)	0.052	24 (11)	25 (15)	0.631
Applied energy (kJ)	222.5 (215.5)	466.7 (300.4)	0.022	98.2 (62.8)	182.4 (140.7)	0.043	127.1 (73.1)	143.7 (87.1)	0.817
Needle positions (n)	3.3 (1.1)	4.2 (2.3)	0.140	4.3 (2.9)	5.2 (3.6)	0.476	3.7 (1.5)	4.0 (2.4)	0.618
Ablation zone volume (mL)	31.6 (13.5-51.7)	54.7 (33.2-67.2)	0.050	69.5 (42.6-96.4)	57.2 (25.8-88.6)	0.548	81.6 (46.6-116.7)	53.3 (21.1-85.6)	0.134
% Tumor of ablation zone volume	15.8 (8.2-22.8)	5.8 (2.8-8.8)	<0.001	18.0 (6.0-30.0)	10.9 (4.4-17.4)	0.178	5.8 (4.6-7.0)	14.9 (13.9-15.9)	0.412
Incomplete after one week of follow-up (n)	2	2	1.000	3	4	0.666	1	2	0.543

*Normally distributed data are presented as mean (SD) and non-normally distributed data are presented as median (Q1-Q3); RFA: radiofrequency ablation; MWA: microwave ablation; HCC: hepatocellular carcinoma; CRLM: colorectal liver metastasis; R(AZ:E): ratio of ablation zone volume to applied energy.

Discussion

The purpose of this study was to find the relation between the amount of applied energy and the resulting ablation zone volume in liver tumors for RFA and MWA devices. To this end we calculated the ratio of ablation zone volume per kJ applied energy. For RFA, R(AZ:E) was approximately similar for HCC and CRLM. Both MWA devices revealed a higher R(AZ:E) in HCC as compared to CRLM; about twofold higher and about 50% higher, for MWA devices A and B, respectively.

The HCCs selected for this study were all in patients with cirrhotic livers, whereas the patients with CRLMs had otherwise healthy livers. The difference in observed treatment effects between the two tumor types can be caused by differences in tumor characteristics and surrounding liver parenchyma associated with the underlying liver

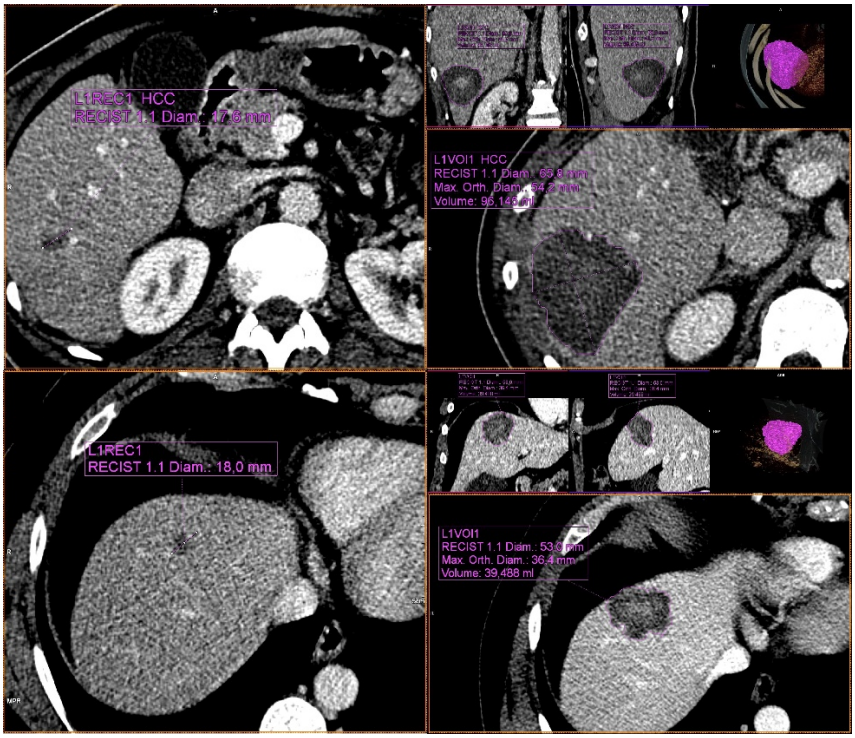

Fig. 2 Left: Preprocedural portal venous phase contrast enhanced CT images of HCC in segment 6 (top) and CRLM in segment 4 in two patients who had not received systemic therapy or transarterial (chemo)embolization. Using MWA device B, 96 kJ (100 W for 8:00 min × 2) and 96 kJ (100 W for 6:00 min, 100 W for 10:00 min) were applied to the HCC and CRLM, respectively, with 16 mm and 14 mm between the two positions of the ablation center of the antenna, so overlap was approximately similar. Right: Resulting ablation zones after segmentation on the 1-week follow-up portal venous phase contrast-enhanced CT images using the MM Oncology package (syngo-via; Siemens, Erlangen, Germany), with ablation zone volumes of 96 mL and 39 mL, resulting in energy deposition ratios of 1.00 mL/kJ and 0.41 mL/kJ for HCC and CRLM, respectively. After 6 months of follow-up, the HCC showed no sign of recurrence, whereas a PET scan of the CRLM showed activity at the dorsal side of the ablation zone, for which reablation was performed

disease. Probably, all of these factors contribute to the differences measured. The underlying mechanisms might be due to differences in electrical properties (relative permittivity and electrical conductivity) and/or thermal properties (thermal conductivity, specific heat capacity, density and nominal blood perfusion rate). Deshazer et al. recently investigated the effect of these properties on the resulting microwave ablation zone in a two-compartment (tumor and surrounding liver parenchyma) computer model [11]. They concluded that changes in characteristics of tumor type had a minimal effect on the ablation zone; the predominant factors influencing the ablation zone were changes in thermal conductivity and hepatic perfusion of the surrounding liver parenchyma. In our study, most of the ablated tissue volume was liver parenchyma and less than 20% consisted of tumor. This seemingly low ratio can be explained by the example that the volume of a spherical 10 mm tumor would only be 12.5% of the total ablation zone volume, if a perfect 5mm safety margin was created around the tumor. This low tumor percentage supports the findings by Delhazer et al.: the main factor influencing treatment effect between tumor types is a difference in tissue characteristics between normal and cirrhotic liver parenchyma. Another variable could be the difference in total liver blood flow in normal livers (with CRLM) versus cirrhotic livers (with HCC). Although some studies found an increase in total liver blood flow in cirrhotic livers [12], most studies agree that cirrhotic liver parenchyma is less perfused compared to normal liver parenchyma [13, 14]. According to the model, a decrease in liver perfusion from 18 (normal) to 11 $kg.m^{-1}s^{-1}$ (cirrhotic) would result in an increase in ablation zone volume of 37% [11]. This corresponds approximately to our results of MWA devices.

Another cause of differences in energy deposition between HCC and CRLM could be caused by the HCC's pseudocapsule. This pseusocapsule has been described as a reason for a hypothetical "oven-effect" to occur: higher temperatures inside the tumor, but lower temperatures outside because of the low thermal conductivity of the capsule. For RFA, it remains to be seen how much heat this capsule actually helps to contain. For MWA, this oven-effect is less likely to occur, as MWA does not rely on thermal conductivity the way RFA does. More detail about the technical differences between MWA and RFA in HCC can be found in a review paper, by Poggi et al [15]. Since the observed difference in ablative effects between HCC and CRLM in this study only occurred with MWA, it is not likely that the "oven-effect" was a significant contributor.

For RFA, the size of the umbrella array significantly affected the ratio of energy deposition. The larger arrays resulted in a lower R(AZ:E). This might be because smaller needle arrays have a better energy deposition, or because the larger arrays have relatively more overlap when performing ablation at multiple locations and thereby losing energy deposition efficiency. For both tumor types the median RFA antenna size was similar, so it is unlikely that this has contributed to how tumor type affects the ratio of energy deposition.

To our knowledge, there is only one clinical study comparing the correlation of applied energy and ablation zone size for HCCs and CRLMs, in MWA [16]. This study generated conflicting results; for shorter ablation times they found no difference in effect, and for longer ablation times they found smaller ablation diameters in HCC versus metastases. They did, however, not measure the volume of the ablation zone, but only diameters.

These were all procedures with a single insertion and energy delivery. No overlapping ablations were included, whereas most of the procedures in this study were performed with overlapping ablations, which might be a reason for the observed differences in outcome.

Lu et al. investigated the effect of flow heat-sink and found that the presence of large (>3mm) peritumoral vessels resulted in a higher ablation site recurrence rate of malignancy after RFA of liver tumors [8]. This heat-sink can be expected to affect the amount of energy required to achieve a certain ablation volume. In our study, this effect was demonstrated for MWA device A with a lower R(AZ:E) for the tumors with peritumoral vascularity, compared to the non-peritumoral vascular tumors. In the RFA and MWA B groups there was no difference in R(AZ:E) between these tumors. MWA B utilizes thermal-, field-, and wavelength control in an effort to produce spherical ablation zones, which might have contributed to the apparent insensitivity to heat-sink [17]. The fact that no heatsink effects were observed in the RFA group is somewhat unexpected and may be because only eight out of thirty tumors in that group were classified as potentially 'high' heat sink tumors.

Although both MWA devices operate in the 2.45 GHz frequency range, their level of power output differs – MWA A generates more power compared to MWA B. It is unclear how much of this power is actually transferred into the tissue, as this is also dependent on the energy reflection of the cable and antenna. However, for MWA A, the transferred power was probably higher and the duration was certainly shorter than for MWA B. Studies investigating the effect of difference in level of power output generally compare between 915 MHZ and 2.45 GHz devices [18, 19]. So, it is unclear how this might have affected observed differences between both MWA devices.

There are some limitations to this study. Often a roundness index is used in order to quantify the quality of the ablation properties of a system [20]. This is because spherical ablation zones are easier to predict and can potentially cover a tumor better than ovoid ablation zones. In this study however, 95% of the tumors were treated at multiple needle positions which meant that a roundness index of the entire ablation zone volume would not be an accurate measure. The latter also means that the amount of overlap could have contributed to differences in volume-energy relation, because the electrical and thermal properties of tissues change after ablation. We could not determine the amount of overlap in the procedures and were not able to compensate for this. Despite this, mean lesion diameter, the number of needle positions, as well as the ablated tumor volume as a percentage of the total volume was not different for the three devices or between tumor types for the MWA devices. Therefore, it is not likely that the amount of overlap was any different between these groups either. Additionally, the non-geometric configuration of the ablation zones was taken into account by a precise volume evaluation of the ablation zone. Finally, histology of adjacent liver parenchyma was not performed, since it is not clinical practice to perform biopsies, neither of the tumor nor of the liver, because diagnosis of both is mainly determined based on medical history of the patient, laboratory results and radiological imaging.

In conclusion, we found a difference in the obtained ablation zone volume per kJ applied energy between tumor types for MWA devices. Because HCCs require less energy to

achieve a certain ablation volume, CRLMs must either be treated by creating multiple ablations with plenty of overlap, or at a relatively higher power level or for a longer time. These data clearly demonstrate that the manufacturers' algorithms solely based on power level and duration of application need adaptation to the type of tumor in its specific environment. Therefore, it remains critical to verify the dimensions of the ablation zone on short term follow-up, using contrast-enhanced CT or preferably contrast enhanced magnetic resonance imaging.

References

1. Curley SA, Izzo F, Delrio P, et al. (1999) Radiofrequency ablation of unresectable primary and metastatic hepatic malignancies: results in 123 patients. Ann Surg 230:1–8
2. Tanis E, Nordlinger B, Mauer M, et al. (2014) Local recurrence rates after radiofrequency ablation or resection of colorectal liver metastases. Analysis of the European Organisation for Research and Treatment of Cancer #40004 and #40983. Eur J Cancer 50:912–9 . doi: 10.1016/j.ejca.2013.12.008
3. Seror O, N'Kontchou G, Nault J-C, et al. (2016) Hepatocellular Carcinoma within Milan Criteria: No-Touch Multibipolar Radiofrequency Ablation for Treatment—Long-term Results. Radiology 150743 . doi: 10.1148/radiol.2016150743
4. Kao W-Y, Chiou Y-Y, Hung H-H, et al. (2011) Risk factors for long-term prognosis in hepatocellular carcinoma after radiofrequency ablation therapy: the clinical implication of aspartate aminotransferase-platelet ratio index. Eur J Gastroenterol Hepatol 23:528–36 . doi: 10.1097/MEG.0b013e328346d529
5. Lam VW-T, Ng KK, Chok KS-H, et al. (2008) Incomplete ablation after radiofrequency ablation of hepatocellular carcinoma: analysis of risk factors and prognostic factors. Ann Surg Oncol 15:782–90 . doi: 10.1245/s10434-007-9733-9
6. Hof J, Wertenbroek MWJLAE, Peeters PMJG, Widder J, Sieders E, de Jong KP (2016) Outcomes after resection and/or radiofrequency ablation for recurrences after treatment of colorectal liver metastases. Br J Surg. doi: 10.1002/bjs.10162
7. Lam VW-T, Ng KK-C, Chok KS-H, et al. (2008) Risk factors and prognostic factors of local recurrence after radiofrequency ablation of hepatocellular carcinoma. J Am Coll Surg 207:20–9 . doi: 10.1016/j.jamcollsurg.2008.01.020
8. Lu DSK, Raman SS, Limanond P, et al. (2003) Influence of Large Peritumoral Vessels on Outcome of Radiofrequency Ablation of Liver Tumors. J Vasc Interv Radiol 14:1267–1274 . doi: 10.1097/01.RVI.0000092666.72261.6B
9. Kim Y, Rhim H, Cho OK, Koh BH, Kim Y (2006) Intrahepatic recurrence after percutaneous radiofrequency ablation of hepatocellular carcinoma: analysis of the pattern and risk factors. Eur J Radiol 59:432–41 . doi: 10.1016/j.ejrad.2006.03.007
10. Ahmed M, Solbiati L, Brace CL, et al. (2014) Image-guided Tumor Ablation: Standardization of Terminology and Reporting Criteria—A 10-Year Update. Radiology 273:241–260 . doi: 10.1148/radiol.14132958
11. Deshazer G, Merck D, Hagmann M, Dupuy DE, Prakash P (2016) Physical modeling of microwave ablation zone clinical margin variance. Med Phys 43:1764 . doi: 10.1118/1.4942980
12. McAvoy NC, Semple S, Richards JMJ, et al. (2016) Differential visceral blood flow in the hyperdynamic circulation of patients with liver cirrhosis. Aliment Pharmacol Ther 43:947–54 . doi: 10.1111/apt.13571
13. Van Beers BE, Leconte I, Materne R, Smith AM, Jamart J, Horsmans Y (2001) Hepatic perfusion parameters in chronic liver disease: dynamic CT measurements correlated with disease severity. AJR Am J Roentgenol 176:667–73 . doi: 10.2214/ajr.176.3.1760667
14. Hashimoto K, Murakami T, Dono K, et al. (2006) Assessment of the severity of liver disease and fibrotic change: The usefulness of hepatic CT perfusion imaging. Oncol Rep 16:677–83 . doi: 10.3892/or.16.4.677
15. Poggi G, Tosoratti N, Montagna B, Picchi C (2015) Microwave ablation of hepatocellular carcinoma. World J Hepatol 7:2578–89 . doi: 10.4254/wjh.v7.i25.2578
16. Amabile C, Ahmed M, Solbiati L, et al. (2017) Microwave ablation of primary and secondary liver tumours: ex vivo, in vivo , and clinical characterisation. Int J Hyperth 33:34–42 . doi: 10.1080/02656736.2016.1196830
17. Berber E (2016) Laparoscopic microwave thermosphere ablation of malignant liver tumors : an initial clinical evaluation. Surg Endosc 30:692–698 . doi: 10.1007/s00464-015-4261-3
18. Simo KA, Tsirline VB, Sindram D, et al. (2013) Microwave ablation using 915-MHz and

2.45-GHz systems: what are the differences? HPB 15:991–996 . doi: 10.1111/hpb.12081

19. Liu F-Y, Yu X-L, Liang P, Wang Y, Zhou P, Yu J (2010) Comparison of percutaneous 915 MHz microwave ablation and 2450 MHz microwave ablation in large hepatocellular carcinoma. Int J Hyperth 26:448–455 . doi: 10.3109/02656731003717574

20. Zaidi N, Okoh A, Yigitbas H, Yazici P, Ali N, Berber E (2016) Laparoscopic microwave thermosphere ablation of malignant liver tumors: An analysis of 53 cases. J Surg Oncol 113:130–4 . doi: 10.1002/jso.24127